

Nonlinear viscoelastic analysis of the torque, axial normal force, and volume change measured simultaneously in the National Institute of Standards and Technology torsional dilatometer

Carl R. Schultheisz^{a)}

Polymers Division, National Institute of Standards and Technology, 100 Bureau Drive, Stop 8544, Gaithersburg, Maryland 20899-8544

Gregory B. McKenna^{b)}

Department of Chemical Engineering, Texas Tech University, P.O. Box 43121, Lubbock, Texas 79409-3121

(Received 18 September 2001; final revision received 1 March 2002)

Synopsis

For compressible materials, the mechanical response to a torsional deformation (at sufficiently large levels of deformation) includes the nonlinear effects of a compressive normal force along the axis of the cylinder and a radial expansion of the cylinder, in addition to the expected torque response. The National Institute of Standards and Technology torsional dilatometer [Duran and McKenna, (1990)] has been used to measure simultaneously the torque, the axial normal force, and the volume change in response to a torsional deformation. In stress-relaxation experiments with an epoxy cylinder just below its glass transition temperature, the torque and normal force decay monotonically, but the volume change associated with the torsion shows an extended relaxation behavior with significant nonmonotonic decay at the lowest temperature investigated. The measurements are modeled with a series solution for torsion of an elastic, compressible material [Murnaghan (1951)]. The elastic solution is adapted for viscoelastic behavior by assuming that isochronal data can be treated as equilibrium elastic data, following a suggestion of Rivlin (1956). © 2002 The Society of Rheology. [DOI: 10.1122/1.1475980]

I. INTRODUCTION

The nonlinear mechanical behavior of polymeric glasses is a field of study that has eluded complete understanding for a variety of reasons. For example, cooling an amorphous material below its glass transition temperature (T_g) places it in a state that is not in thermodynamic equilibrium. If the glass is then held at a temperature below T_g , the structure of the material evolves slowly toward equilibrium. This evolution can be observed in measurements of different properties of the material, such as the volume, enthalpy, optical behavior, or the mechanical response of the material [Kovacs (1963); Struik (1978); Kovacs *et al.* (1979); Scherer (1986); McKenna (1989); Hodge (1994); Mijovic *et al.* (1994)]. In such aging experiments, the ability to make simultaneous measurements on a single sample eliminates any questions of differences between samples or

^{a)}Current affiliation: National Transportation Safety Board, Washington, D.C. 20594.

^{b)}Author to whom correspondence should be addressed; electronic mail: greg.mckenna@coe.ttu.edu

differences in thermal histories. The National Institute of Standards and Technology (NIST) torsional dilatometer [Duran and McKenna (1990); Santore *et al.* (1991); McKenna *et al.* (1994; 1995); Schultheisz *et al.* (1995)] can be used to make such simultaneous measurements of the torque, the axial normal force, and the change in volume of a cylindrical sample in response to an applied twist and/or a change in temperature. These capabilities have been very useful in comparing the evolution of the sample volume and the mechanical response of glassy polymers in physical aging experiments. The current work focuses, however, on a series of experiments using the NIST torsional dilatometer that were performed on an epoxy glass that was aged into thermodynamic equilibrium prior to performing the mechanical measurements.

In the present paper, we are interested in the nonlinear viscoelastic response of a cylinder held at constant length and twisted to a fixed angle of twist. In particular, we have observed an apparently anomalous nonmonotonic relaxation of the cylinder's volume change, and we examine the possibility that this nonmonotonic behavior can be described within a viscoelastic extension of the Murnaghan (1951) series solution for the torsion of a compressible elastic cylinder. The nonmonotonic volume change has not been reported previously. The approach we take to model the deformation is to adapt the finite-deformation analysis of Murnaghan (1951) to isochronal viscoelastic behavior. This is also new. The main question we address is whether the model can capture the differences in the observed behaviors using reasonable physical assumptions. The model is successful to the extent that it suggests that the differences in the relaxation of the torque, normal force, and volume change resulting from a torsional deformation are allowable within the context of the theory, while the viscoelastic modulus functions involved are well-behaved and relax monotonically. The nonmonotonic volume change results from differences in the rate of relaxation of different modulus functions. Within the context of finite deformation elasticity theory, the problem of torsion of a circular cylinder (or tube) has been investigated for both incompressible materials [Rivlin (1948); Penn and Kearsley (1976)] and compressible materials [Rivlin (1948); Murnaghan (1951); Green (1955); Levinson (1972); Wack (1981, 1989); Wu and van der Giessen (1993); Wineman and McKenna (1996)]. Penn and Kearsley (1976) showed that, for an incompressible material, measurements of the torque and normal force as a function of angle of twist were sufficient to determine the derivatives of the strain energy function with respect to the first two strain invariants (the third invariant being a constant for incompressible materials). Their approach relied upon the fact that a cylinder made of an incompressible material occupies the same space in both the undeformed and deformed configurations when only torsion is involved. It was originally thought that the three measurements of the torque, normal force, and volume change (radial expansion) in the NIST torsional dilatometer would be sufficient to determine the derivatives of the strain energy function with respect to all three of the strain invariants for the case of elastic compressible materials. However, Wineman and McKenna (1996) recently concluded that such a determination was not possible. While the measurement of the volume change would identify the radial position of the outside surface of the cylinder, the radial displacement in the interior of the cylinder would follow an unknown function that depends on the material properties, so that the approach used by Penn and Kearsley (1976) for the incompressible material would not work. The measurements of the torque, normal force, and volume change are therefore insufficient to determine directly the derivatives of the strain energy function with respect to the strain invariants for a compressible material. Wineman and McKenna (1996) suggest that one way to proceed would be to assume a form for the strain energy function (such as a polynomial in the strain invariants) and determine the parameters in the function by a minimization of the difference between

measured and calculated quantities. For the analysis in this paper, we have adopted the truncated series expansion for the torsion of an isotropic, homogeneous, elastic, compressible cylinder developed by Murnaghan (1951). This choice leads to a polynomial expansion of the strain energy function in terms of the strain invariants, similar to the suggestion of Wineman and McKenna (1996). Murnaghan's formulation of the torsion problem leads to a solution in terms of the Lamé constants λ and μ , and two higher-order moduli denoted m and n . The three measurements of torque, normal force, and volume change are sufficient to determine μ and n uniquely, but λ and m cannot be uniquely determined. The problem is additionally complicated by the time-dependent nature of the response to the twist. We follow Rivlin (1956) in assuming that, for isochronal data obtained from single-step stress relaxation experiments, the results of the elastic analysis can be extended to the viscoelastic case by replacing the elastic moduli λ , μ , m , and n with functions of time t and temperature T , indicated by $\lambda(t, T)$, $\mu(t, T)$, $m(t, T)$ and $n(t, T)$. We assume that these modulus functions are monotonically decaying functions of time, and that the shifts in the relaxation times have a common dependence on temperature. The adaptation of an elastic analysis to isochronal viscoelastic behavior using the assumption of Rivlin (1956) was originally employed by McKenna and Zapas (1985) in analyzing the torsion problem. In other work, Pesce and McKenna (1997) used the incompressible solution to estimate the strain energy function for a compressible polymer glass in order to go from torsional measurements to extension and compression deformation geometries.

In the experiments described in this paper and in other experiments with this epoxy [Duran and McKenna (1990); Santore *et al.* (1991); McKenna *et al.* (1994, 1995); Schultheisz *et al.* (1995)], the application of the torsional deformation has always led to an increase in the sample volume, which then relaxes. A result from the aging experiments indicates that the volume increase caused by the twist eventually relaxes to zero, although the torque and normal force relax to nonzero rubbery modulus values. One might anticipate this behavior, arguing that since the shear modulus decreases much more than the bulk modulus, then at long times the polymer appears more like an incompressible material. Within the context of the model based on the analysis of Murnaghan (1951), however, the situation is slightly more complex, in that this behavior implies that the long-term values of the modulus functions are related and combine to make the volume change relax to zero.

While the experiments with epoxy in the NIST torsional dilatometer [Duran and McKenna (1990); Santore *et al.* (1991), McKenna *et al.* (1994, 1995); Schultheisz *et al.* (1995)] have consistently shown an increase in the sample volume in response to a twist, other researchers have obtained different results on other materials tested in torsion using slightly different boundary conditions. Wang *et al.* (1982) report data for poly(methyl methacrylate), polycarbonate, poly(tetrafluoroethylene), and an acetal copolymer, tested at room temperature under torsion at a constant angular rate. However, unlike our experiments, the specimen length in those experiments was not constrained. All four polymers tested by Wang *et al.* (1982), showed an increase in length and a decrease in radius (as measured by dial gauge and an extensometer, respectively) with increasing angle of twist per unit length. The net volume increased for the acetal copolymer, but decreased for the other three materials. Pixa *et al.* (1988) studied unplasticized poly(vinyl chloride) apparently at room temperature using an apparatus similar to the one used for our experiments, except that again the specimen was free to extend along its length. They also found that the volume decreased upon imposition of a small torsional deformation, but as the level of deformation increased, the volume began to increase back toward its initial value. No significant stress relaxation or volume change was found for small deforma-

tions, but at a strain of 14.8%, they indicate modest stress relaxation, and a volume shift downward. {Such densification under an applied deformation well below T_g has also been reported for polycarbonate [Smith *et al.* (1988); Colucci *et al.* (1997)].} Murnaghan (1951) noted that his solution for the torsion of a cylinder would allow for either a volume increase or a volume decrease, depending on the relative magnitude and sign of the various moduli, and the response might depend on the boundary condition regarding the freedom of the cylinder length to change. The range of behavior would also be constrained by restrictions on the strain energy function, which would bound the moduli [Wineman and McKenna (1996); Baker and Ericksen (1954)].

In this paper, we investigate the torque, normal force, and volume change using data from experiments in which the material has been aged into equilibrium at three different temperatures. We model the behavior using a viscoelastic extension of the elastic analysis of Murnaghan (1951) within a framework that imposes the same time-temperature superposition for all four modulus functions. This constraint is intended to ensure that the strain energy function has a unique temperature dependence. The shear modulus $\mu(t, T)$ can be calculated directly from the measured torque, and it is modeled very well using a single stretched exponential function and time-temperature superposition. The higher-order modulus function $n(t, T)$ can also be calculated directly from the measurements. We assume a form for $\lambda(t, T)$ that is related to $\mu(t, T)$, and then investigate the calculated $m(t, T)$. Each modulus function is modeled with a single stretched exponential function incorporating time-temperature superposition using the same shift factors as $\mu(t, T)$. Much of the observed behavior can be captured with this restricted model, but the results suggest that the higher-order modulus functions may not follow the same time-temperature shift behavior as $\mu(t, T)$, or that a secondary relaxation behavior is present in the higher-order modulus functions, but does not appear in the shear modulus. Without a separate measurement to decouple $\lambda(t, T)$ from $m(t, T)$, however, this issue is unresolved.

II. EXPERIMENT

The NIST torsional dilatometer is described in detail in the paper by Duran and McKenna (1990). The material is a diglycidal ether of bisphenol-A epoxy, cured with a flexible poly(propylene oxide) diamine with a molecular mass of 400 g/mol, giving a nominal glass transition temperature of 42.4 °C [Lee and McKenna (1988)]. Use of a thermoset is intended to allow repeated experiments on the same sample. The epoxy and curing agent were mixed, poured into a glass tube mold, and then degassed under vacuum. The epoxy was cured at 100 °C for 24 h, and the sample was then bonded with thin layers of a filled epoxy automotive adhesive between two stainless-steel end grips aligned in V blocks on a machinist's flat. We assume that the influence of the adhesive bonding the specimen to the grips is negligible, since it is filled, has a much higher glass transition than the sample, and occupies less than 1% of the volume of the sample. The grips are 25.54 mm in diameter with a standard uncertainty of 0.01 mm. The test section of the sample was turned on a lathe to a uniform diameter of 15.22 mm (standard uncertainty 0.05 mm), with a length of 115.1 mm (standard uncertainty 0.5 mm). Outside the test section was left a disk of epoxy approximately 1 mm thick at each end having the same diameter as the grips; the radius of curvature of the fillet between the test section and each end piece was specified to be 1.6 mm.

One specimen grip attaches to a torque and normal force transducer, and the other grip attaches to a servo motor, which is used to apply a constant angle of twist for stress relaxation experiments. The angle of twist per unit length applied in these experiments

was 3.94 rad/m with a standard uncertainty of 0.05 rad/m. The shear strain varies linearly with the radius, and this amount of twist leads to a shear strain of 0.0300 (standard uncertainty 0.0004) at the outer radius of the sample. The specimen was sealed into a stainless-steel chamber, and the remainder of the chamber was first evacuated and then filled with 586 g (standard uncertainty 1 g) of mercury. The dilatometer chamber is connected to a vertical precision capillary, into which the mercury is free to flow. The core of a linear variable differential transformer is attached to a poly(methyl methacrylate) float that sits on top of the mercury in the capillary to measure the mercury level and thus determine the change in the volume of the specimen in the dilatometer. The temperature within the dilatometer chamber is controlled by circulating fluid from a constant-temperature bath through copper coils wrapped around the chamber containing the sample and the mercury. The temperature within the dilatometer chamber is monitored using a platinum resistance thermometer. Over the course of an entire aging experiment (several days to two weeks), the standard uncertainty in the dilatometer temperature after thermal equilibration is 0.01 °C. For the experiments investigated in this paper, which occupy a much shorter time of a single twist step (several hours to less than 2 days), the standard uncertainty in the dilatometer temperature can be as small as 0.003 °C. The entire instrument, including the motor, the dilatometer chamber and the torque/normal force cell, are also isolated from the room environment within an enclosure where the temperature is controlled at 29.2 °C (with standard uncertainty 0.2 °C). The standard uncertainty in the torque measurement is 0.05 N m; the standard uncertainty in the normal force measurement is 1 N; and the standard uncertainty in the volume measurement is $2 \times 10^{-5} \text{ cm}^3$.

The experiments described here are single torsional stress relaxation experiments for samples that were aged into equilibrium. For consistency, the three experiments analyzed were all for samples equilibrated after up-jumps of approximately 2 °C, with final temperatures of 37.93, 35.51, and 32.80 °C.

Following Kovacs (1963) and Kovacs *et al.* (1979), the volume measurements in the aging experiments were put into a normalized form given the symbol $\delta(t, T)$, which is the relative deviation of the volume from a reference value, with

$$\delta(t, T) = \frac{V(t, T) - V_{\text{ref}}(T)}{V_{\text{ref}}(T)}, \quad (1)$$

where $V(t, T)$ is the current volume at time t and temperature T , and $V_{\text{ref}}(T)$ is the reference volume at temperature T . This normalized form is retained for describing the volume change caused by the torsional deformation, in which case $V_{\text{ref}}(T)$ is the volume in the initial, undeformed reference configuration. Thus, $\delta(t, T)$ is effectively a volumetric strain measure. Because the measurements of the response to the torsion in the present paper were made after the sample had reached thermodynamic equilibrium, the reference volume $V_{\text{ref}}(T)$ is equal to the volume at thermodynamic equilibrium, $V_{\infty}(T)$, which is the quantity of interest in the aging experiments. With the cylinder ends constrained so that it cannot change length, $\delta(t, T)$ is directly related to the change in the cylinder radius from its undeformed, reference value, and $\delta(t, T)$ can therefore be used as a normalized measure of the change in the outer radius of the cylinder for the deformed configuration compared to the initial undeformed reference configuration. Radial constraints at the grips are neglected in this initial analysis. The standard uncertainty in $\delta(t, T)$ is governed mainly by the standard uncertainty in the temperature. Based on the parameters of the measurement system alone, the standard uncertainty in each measurement of $\delta(t, T)$

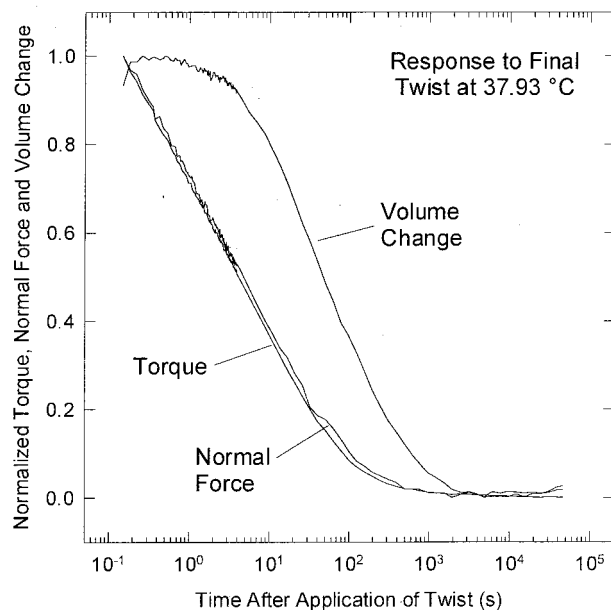


FIG. 1. Normalized relaxation responses for torque, normal force, and volume change in response to a twist at 37.93 °C. Responses were normalized to vary from 0 to 1 by their maximum and minimum values.

would be on the order of 10^{-6} . Taking the standard uncertainty in the temperature during a single twist as 0.003 °C, a calculation of the propagation of uncertainties using the density of mercury as a function of temperature [CRC Handbook (1997)] and the liquid coefficient of thermal expansion of the epoxy, $\alpha_L = 5.9 \times 10^{-4} \text{ cm}^3/(\text{cm}^3 \text{ K})$ [Duran and McKenna (1990)], we obtain an estimate of the standard uncertainty in $\delta(t, T)$ of 3×10^{-6} . Over the course of an entire aging experiment, with the standard uncertainty in the temperature equal to 0.01 °C, the standard uncertainty in δ is 10^{-5} . This result is somewhat better than the uncertainty estimated for the classical dilatometer measurements of Kovacs and coworkers [Kovacs (1963); Kovacs *et al.* (1979); Struik (1997a, 1997b); McKenna *et al.* (1999)].

Figures 1, 2, and 3 show torque, normal force, and volume responses to a twist at three different temperatures. The data were normalized to lie between 0 and 1 using the maximum and minimum values, in order to show the different time dependence of each response. The normal force is compressive, and taken as negative in the convention used in this paper, so those data have actually been inverted. The volume has always been observed to increase under torsion with this material. The choice of positive or negative for the torque is arbitrary. The data in Fig. 1 are for a jump from 36.01 to 37.93 °C. The data in Fig. 2 are for a jump from 33.52 to 35.51 °C. The data in Fig. 3 are for a jump from 30.80 to 32.80 °C. The origin for the time in Figs. 1–3 was taken to be halfway between the last data point before the twist was applied and the data point at which the torque reached its maximum [Zapas and Craft (1965); Santore *et al.* (1991)]. The rise time for the torque averaged 0.28 s (standard uncertainty 0.05 s). In magnitude, the maximum torque is on the order of 15 N m, the maximum normal force is on the order of 80 N, and the maximum $\delta(t, T)$ is on the order of 2×10^{-4} . At 37.93 °C, the torque and normal force relaxations are almost identical, but at the lower temperatures, the normal force relaxation trails the torque relaxation somewhat. The volume response is considerably

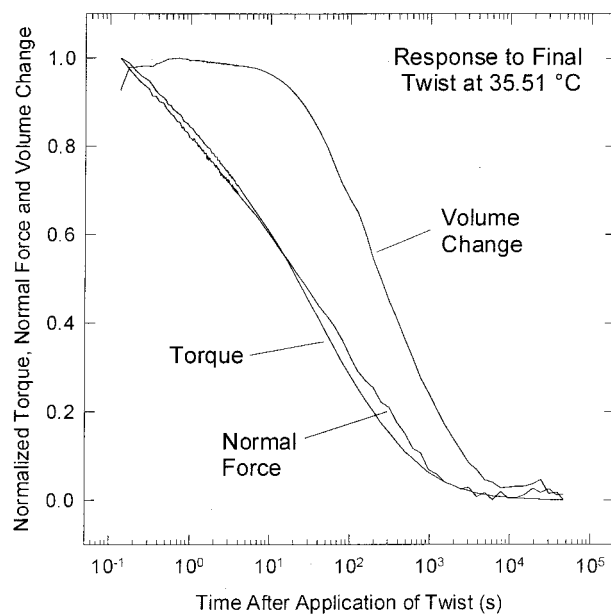


FIG. 2. Normalized relaxation responses for torque, normal force and volume change in response to a twist at 35.51 °C. Responses were normalized to vary from 0 to 1 by their maximum and minimum values.

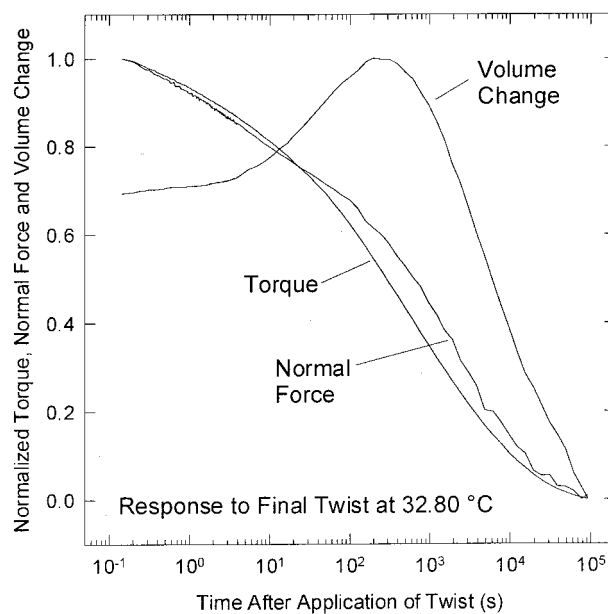


FIG. 3. Normalized relaxation responses for torque, normal force, and volume change in response to a twist at 32.80 °C. Responses were normalized to vary from 0 to 1 by their maximum and minimum values.

different from the torque or normal force in all three sets of data, but the nonmonotonic behavior of the volume response at 32.80 °C is the most striking. In chronological order, the up-jump experiment to 35.51 °C (Fig. 2) was first, followed by the up-jump experiment to 32.80 °C (Fig. 3) and then the up-jump experiment to 37.93 °C (Fig. 1). This sequence indicates that the nonmonotonic behavior of the volume is only a function of temperature, and is not an indication of a problem with the dilatometer. In subsequent experiments moving to lower temperatures, the nonmonotonic volume response again appeared. A model to describe this behavior is presented in the following section.

III. ANALYSIS OF THE TORSIONAL DEFORMATION: MURNAGHAN'S SERIES SOLUTION

The nonlinear material behaviors (axial normal force and volume change) from the three experiments shown in Figs. 1, 2, and 3 were investigated using an adaptation of the truncated series expansion developed by Murnaghan (1951) for the torsion of an isotropic, homogeneous, elastic, compressible material. Murnaghan actually provides the solution for the case where the ends of the cylinder are free to move, but incorporating the boundary condition fixing the length of the cylinder is straightforward. Murnaghan's notation for the problem is slightly different from that of Rivlin (1948), which has commonly been adopted by subsequent researchers for investigations of the torsion of both incompressible and compressible materials [Green (1955); Levinson (1972); Penn and Kearsley (1976); Wineman and McKenna (1996); Pesce and McKenna (1997)]. Given the deformation gradient tensor \mathbf{F} , the traditional formulation develops the analysis in terms of the right Cauchy–Green strain tensor $\mathbf{C} = \mathbf{F}^T \mathbf{F}$ [Spencer (1980)]. For an isotropic, homogeneous material, the stress is a function only of the three invariants of \mathbf{C} : I_1 , I_2 , and I_3 , with

$$\begin{aligned} I_1 &= \text{tr } \mathbf{C} = \lambda_1^2 + \lambda_2^2 + \lambda_3^2, \\ I_2 &= \frac{1}{2}[(\text{tr } \mathbf{C})^2 - \text{tr}(\mathbf{C}^2)] = \lambda_1^2 \lambda_2^2 + \lambda_2^2 \lambda_3^2 + \lambda_1^2 \lambda_3^2, \\ I_3 &= \det \mathbf{C} = \lambda_1^2 \lambda_2^2 \lambda_3^2, \end{aligned} \quad (2)$$

where λ_1 , λ_2 , and λ_3 are the principal stretches associated with the deformation gradient tensor \mathbf{F} . The Cauchy stress is denoted by \mathbf{T} and can be calculated as

$$\mathbf{T} = 2 \frac{\rho}{\rho_0} \mathbf{F} \left[\frac{\partial W}{\partial I_1} \mathbf{I} + \frac{\partial W}{\partial I_2} (I_1 \mathbf{I} - \mathbf{C}) + \frac{\partial W}{\partial I_3} (I_2 \mathbf{I} - I_1 \mathbf{C} + \mathbf{C}^2) \right] \mathbf{F}^T, \quad (3)$$

where $W(I_1, I_2, I_3)$ is the strain energy potential, \mathbf{I} is the identity tensor, ρ is the density of the deformed body, and ρ_0 is the density of the undeformed body [Spencer (1980)]. Note that $\rho/\rho_0 = I_3^{-1/2}$. Also note that carrying out the tensor multiplications with \mathbf{F} and \mathbf{F}^T recasts the stress tensor in terms of the left Cauchy–Green strain tensor \mathbf{B} , since $\mathbf{B} = \mathbf{F} \mathbf{F}^T$ (also, $\mathbf{B}^2 = \mathbf{F} \mathbf{C} \mathbf{F}^T$ and $\mathbf{B}^3 = \mathbf{F} \mathbf{C}^2 \mathbf{F}^T$) [Spencer (1980)]; the invariants of \mathbf{B} and \mathbf{C} are the same. The comparison with Murnaghan's analysis is more straightforward using Eq. (3). Murnaghan (1951) formulates the problem using a strain tensor $\boldsymbol{\eta} = (\mathbf{C} - \mathbf{I})/2$. The principal axes of $\boldsymbol{\eta}$ and \mathbf{C} are the same. If we denote the invariants of $\boldsymbol{\eta}$ as J_1 , J_2 , and J_3 , we get very similar equations for the invariants and the Cauchy stress as a function of $\boldsymbol{\eta}$:

$$\begin{aligned}
 J_1 &= \text{tr } \boldsymbol{\eta}, \\
 J_2 &= \frac{1}{2}[(\text{tr } \boldsymbol{\eta})^2 - \text{tr}(\boldsymbol{\eta}^2)], \\
 J_3 &= \det \boldsymbol{\eta}.
 \end{aligned} \tag{4}$$

The Cauchy stress is then

$$\mathbf{T} = 2 \frac{\rho}{\rho_0} \mathbf{F} \left[\frac{\partial W}{\partial J_1} \mathbf{I} + \frac{\partial W}{\partial J_2} (J_1 \mathbf{I} - \boldsymbol{\eta}) + \frac{\partial W}{\partial J_3} (J_2 \mathbf{I} - J_1 \boldsymbol{\eta} + \boldsymbol{\eta}^2) \right] \mathbf{F}^T. \tag{5}$$

Murnaghan thus develops his solution in terms of $\boldsymbol{\eta}$, J_1 , J_2 , and J_3 , but the solution can be transformed into the other notation very easily, because the two strain tensors have a simple relation and the invariants are also related

$$\begin{aligned}
 J_1 &= \frac{1}{2}(I_1 - 3), \\
 J_2 &= \frac{1}{4}(I_2 - 2I_1 + 3) = \frac{1}{4}[(I_2 - 3) - 2(I_1 - 3)], \\
 J_3 &= \frac{1}{8}(I_3 - I_2 + I_1 - 1) = \frac{1}{8}[(I_3 - 1) - (I_2 - 3) + (I_1 - 3)], \\
 I_1 &= 2J_1 + 3, \\
 I_2 &= 4J_2 + 4J_1 + 3, \\
 I_3 &= 8J_3 + 4J_2 + 2J_1 + 1.
 \end{aligned} \tag{6}$$

Rivlin (1953) used similar notation in a brief paper suggesting a formalism for solving boundary value problems using Murnaghan's second order elasticity theory. Murnaghan expands the strain energy potential $W(J_1, J_2, J_3)$ as an infinite series in the arguments J_1 , J_2 , and J_3 . In the undeformed state, $\boldsymbol{\eta} = \mathbf{0}$, and the series expansion can be understood as an expansion in the components of $\boldsymbol{\eta}$ (which are assumed to be small quantities). The strain invariants are such that J_1 contains only linear combinations of the components of $\boldsymbol{\eta}$, J_2 contains only second order combinations of the components of $\boldsymbol{\eta}$, and J_3 contains only third order combinations of the components of $\boldsymbol{\eta}$. After expanding the strain energy potential $W(J_1, J_2, J_3)$ in powers of J_1 , J_2 , and J_3 , terms are grouped which have combinations of the components of $\boldsymbol{\eta}$ of the same order. For a deformation arising from an initially stress-free state, Murnaghan gives the solution (truncated beyond third order combinations of the components of $\boldsymbol{\eta}$) as

$$W = \frac{\lambda + 2\mu}{2} J_1^2 - 2\mu J_2 + \frac{l + 2m}{3} J_1^3 - 2m J_1 J_2 + n J_3, \tag{7}$$

where λ and μ are the Lamé constants from linearized elasticity theory, and l , m , and n are additional elastic constants governing the nonlinear behavior. The first two terms in Eq. (7) include components of $\boldsymbol{\eta}$ to second order, and truncating the series at that point corresponds to linearized elasticity theory. The next three terms include all combinations of the invariants that include the components of $\boldsymbol{\eta}$ to third order, and Murnaghan truncates his expansion at that point. For comparison, rewriting W in Eq. (7) in terms of the invariants of \mathbf{C} gives

$$\begin{aligned}
W = & \left[\mu + \frac{n}{8} \right] (I_1 - 3) - \left[\frac{\mu}{2} + \frac{n}{8} \right] (I_2 - 3) + \frac{n}{8} (I_3 - 1) + \left[\frac{\lambda + 2\mu}{8} + \frac{m}{2} \right] (I_1 - 3)^2 - \frac{m}{8} (I_1 - 3)(I_2 - 3) \\
& + \left[\frac{l + 2m}{24} \right] (I_1 - 3)^3
\end{aligned} \tag{8}$$

using a form similar to that suggested by Wineman and McKenna (1996). In the undeformed state, $\mathbf{C} = \mathbf{I}$, and $I_1 = 3$, $I_2 = 3$, and $I_3 = 1$, so this expansion is also in terms of small quantities. Note that Eq. (8) is similar to Eq. (7) in that it includes all combinations of components of \mathbf{C} up to the third order. However, Eq. (8) also includes a term with I_1 alone, whereas in Murnaghan's expansion, the term including J_1 alone describes an initial hydrostatic stress that could be present, but is neglected here in assuming an initially stress-free condition. More importantly, if one were to truncate the expansion in Eq. (8) after terms including components of \mathbf{C} up to second order, one would obtain a constitutive relation that is different from linearized elasticity theory, which includes terms containing the moduli λ , μ , m , and n . This result emphasizes the well-known fact that a different choice of a strain measure and a subsequent expansion of the strain energy in the invariants of that strain measure, along with a specific choice for truncation, can lead to a different higher-order constitutive theory. This point was also demonstrated recently by Hoger (1999), who developed a similar expansion based on the Biot strain \mathbf{E} , which can be related to the other strain measures $\boldsymbol{\eta}$ and \mathbf{C} through the equation $\boldsymbol{\eta} = (\mathbf{C} - \mathbf{I})/2 = \mathbf{E}^2/2 + \mathbf{E}$. When the deformation is small enough, both $\boldsymbol{\eta}$ and \mathbf{E} (as well as a number of other commonly used strain measures) are equivalent, and the linearized theory of elasticity is recovered in the different analyses.

Assuming an elastic response, the kinematic description for the problem of torsion of a circular cylinder with no change of length allowed is specified by a mapping from the reference configuration characterized by (R, Θ, Z) to the deformed configuration characterized by (r, θ, z) , with

$$\begin{aligned}
r &= r(R), \\
\theta &= \Theta + \psi Z, \\
z &= Z,
\end{aligned} \tag{9}$$

where ψ is the angle of twist per unit length [Wineman and McKenna (1996)]. The cylinder length is constant, and the angular displacement is a linear function of position along the length of the cylinder. The outer surface of the cylinder is denoted R_0 in the undeformed configuration, and $r_0 = r(R_0)$ in the deformed configuration. Solution of the problem involves determining the function $r(R)$ and the corresponding stress field from the strain energy potential using the equations of equilibrium, with the boundary conditions that the external surface of the cylinder is traction-free and the stress at the center of the cylinder is bounded. Constraints on the radial expansion near the ends of the cylinder imposed by the connection to the grips are neglected in the current analysis.

For this specific problem, Murnaghan's analysis leads to solutions for the moment, normal force and volume as functions of the Lamé constants λ and μ and two of the higher-order elastic constants, m and n . The torsion problem is independent of the elastic constant l . Also, it should be noted that, whereas the shear strain and associated torque are linear in ψ , the volume change and normal force are at least second order effects with

respect to ψ . In calculating the strain tensor, some of these components are multiplied together, and Murnaghan truncates the strain tensor to include components only up to the level of ψ^2 .

In the case of a viscoelastic material, the radial mapping now depends on time and temperature, with $r = r(R, t, T)$. For a single-step, isothermal stress relaxation experiment, Rivlin (1956) has suggested that viscoelastic functions that depend on time and temperature can be substituted for the elastic constants in the solution, giving $\lambda(t, T)$, $\mu(t, T)$, $m(t, T)$, and $n(t, T)$. This approach was earlier used by McKenna and Zapas (1985) to adapt an elastic analysis of the torsion problem to isochronal viscoelastic data. This approach is equivalent to assuming that the deformation can be described by a function that is separable in the time and space variables. Since we have only three measurements, but four unknown functions, we must make an assumption about one of the functions in order to proceed. We approximate $\lambda(t, T)$ using literature values for the bulk modulus and Poisson's ratio to relate $\lambda(t, T)$ to the measured $\mu(t, T)$.

Murnaghan's analysis leads to a specific form for the deformation in Eq. (9) given by

$$\begin{aligned} r &= R + \psi^2 \omega(R, t, T), \\ \theta &= \Theta + \psi Z, \\ z &= Z, \end{aligned} \tag{10}$$

where ψ is the angle of twist per unit length, and the unknown function $\omega(R, t, T)$ is determined by solving the equations of equilibrium with the boundary condition that the radial surface of the cylinder is stress free. In this case, the torsion problem is a mixed boundary value problem, in that the deformation is specified at the ends of the cylinder, but the stress is specified on the radial surface of the cylinder. A typical uniaxial stress relaxation experiment with stress-free lateral surfaces is also a mixed boundary value problem. The relation between the applied moment (or torque) $M(t, T)$ and the shear modulus is the same as that calculated using linear viscoelastic theory, and since we assume that the torsional deformation is applied as a step change, the convolution integral relating the moment and the shear modulus reduces to an algebraic relation, with

$$M(t, T) = \pi R_0^4 \int_0^t \mu(t - \xi, T) \frac{d\psi(\xi)}{d\xi} d\xi = \pi R_0^4 \mu(t, T) \psi. \tag{11}$$

Similarly, the higher-order modulus functions $m(t, T)$ and $n(t, T)$ are only convolved with terms arising from the shear strain (at this level of approximation), so $m(t, T)$ and $n(t, T)$ also only appear in algebraic combinations. Two of the equations of equilibrium are satisfied identically; the remaining equation is

$$\begin{aligned} &\int_0^t [\lambda(t - \xi, T) + 2\mu(t - \xi, T)] \frac{\partial}{\partial \xi} \left[\frac{\partial^2 \omega(R, \xi, T)}{\partial R^2} + \frac{1}{R} \frac{\partial \omega(R, \xi, T)}{\partial R} - \frac{\omega(R, \xi, T)}{R^2} \right] d\xi \\ &= \left[2\mu(t, T) - \lambda(t, T) - m(t, T) + \frac{3}{4} n(t, T) \right] R. \end{aligned} \tag{12}$$

Assuming that $\omega(R, t, T)$ can be written in a form that is separable into a function of R multiplying a function of time and temperature leads to the result

$$\omega(R,t,T) = p_1(t,T)R_0^2R + p_2(t,T)\frac{R_0^4}{R} + p_3(t,T)R^3, \tag{13}$$

where the first two terms represent the homogeneous solution to the differential equation for $\omega(R,t,T)$ in Eq. (12). Since the stress must be bounded at $R = 0$, $p_2(t,T) \equiv 0$. The problem involving torsion of a hollow tube would require all three terms, but also have an additional stress-free boundary condition on the inner surface of the tube. Equation (12) therefore reduces to an equation for $p_3(t,T)$, which is used to simplify the equation for the stress-free boundary condition on the outer surface of the cylinder. Let us define a function $D(t,T)$ as $D(t,T) = 2[r(R_0,t,T) - R_0]/R_0$, which is twice the relative change in the outer cylinder radius from its initial value of R_0 , so $D(t,T) = 2\psi^2R_0^2[p_1(t,T) + p_3(t,T)]$. Since the cylinder length is constrained, $D(t,T)$ is also related to the measured volumetric strain $\delta(t,T)$, with $D(t,T) = 2\{[1 + \delta(t,T)]^{1/2} - 1\}$. To first order, $D(t,T) \approx \delta(t,T)$, and this approximation is very good since $\delta(t,T)$ is on the order of 10^{-4} . Rewriting the condition that the radial boundary is stress free in terms of $D(t,T)$ then gives

$$\int_0^t [\lambda(t-\xi,T) + \mu(t-\xi,T)] \frac{\partial D(\xi,T)}{\partial \xi} d\xi = \frac{\psi^2R_0^2}{16} \{-4[\lambda(t,T) + 2\mu(t,T) + m(t,T)] + n(t,T)\}. \tag{14}$$

The resulting axial normal force averaged over the area of the ends of the cylinder is denoted $N(t,T)$ and is calculated as

$$N(t,T) = -\pi R_0^2 \int_0^t \mu(t-\xi,T) \frac{\partial D(\xi,T)}{\partial \xi} d\xi + \frac{\pi\psi^2R_0^4}{16} n(t,T). \tag{15}$$

Equations (11), (14), and (15) can be arranged to give equations for the modulus functions in terms of the measured quantities, the moment (or torque) $M(t,T)$, the axial normal force $N(t,T)$, and the volumetric strain $\delta(t,T)$, which is related to $D(t,T) = 2\{[(1 + \delta(t,T))^{1/2} - 1]\}$:

$$\mu(t,T) = \frac{2M(t,T)}{\pi\psi R_0^4}, \tag{16}$$

$$n(t,T) = \frac{16}{\psi^2R_0^2} \left[\frac{N(t,T)}{\pi R_0^2} + \int_0^t \mu(t-\xi,T) \frac{\partial D(\xi,T)}{\partial \xi} d\xi \right], \tag{17}$$

$$m(t,T) = \frac{4}{\psi^2R_0^2} \left[\frac{N(t,T)}{\pi R_0^2} - \int_0^t \lambda(t-\xi,T) \frac{\partial D(\xi,T)}{\partial \xi} d\xi \right] - [\lambda(t,T) + 2\mu(t,T)]. \tag{18}$$

The relation in Eq. (16) is the same as that found for linear theory, because the series expansion has been truncated so that there are no additional terms that are odd functions of ψ . Equations (16) and (17) show that $\mu(t,T)$ and $n(t,T)$ can be evaluated directly from measured quantities (with some approximate method of evaluating the convolution integral), but Eq. (18) shows that $\lambda(t,T)$ and $m(t,T)$ can only be expressed in terms of one another. Equations (14) and (15) suggest that the normal force and volumetric strain are functions of more than one modulus function, which provides a mechanism for added

complexity in the relaxation behavior of those quantities. Note that the moment in Eqs. (11) or (16) scales as ψR_0^4 and the normal force in Eq. (15) scales as $\psi^2 R_0^4$ [since $D(t, T)$ scales as $\psi^2 R_0^2$ from Eqs. (10) and (13)], which is the same scaling found by Penn and Kearsley (1976) for incompressible materials.

We now choose a mathematical form for the modulus functions, and attempt to reproduce the measured behavior of the moment, axial normal force and volume change. The moment $M(t, T)$ [and thus the shear modulus $\mu(t, T)$] can be modeled very well by a single stretched exponential function. Based on that result, all four of the modulus functions were modeled using a single stretched exponential function. We also enforce a condition that the relaxation time for each of the four modulus functions is modified by a single temperature shift factor $a(T)$ determined from the fit to the shear modulus data. We also allow a small vertical shift factor for each modulus function, which is constrained to follow a similar behavior with temperature as $a(T)$. Specifically, the shear modulus is written as

$$\mu(t, T) = b(T) \left([\mu_0 - \mu_\infty] \exp \left\{ - \left[\frac{t}{a(T)\tau} \right]^\beta \right\} + \mu_\infty \right), \quad (19)$$

where μ_0 , μ_∞ , β , and τ govern the relaxation at the reference temperature where $a(T) = 1$ and $b(T) = 1$. We use 35.51 °C as the reference temperature. The temperature range across the three experiments is small, so it is expected that both $\log[a(T)]$ and $\log[b(T)]$ would be approximated well by linear functions of temperature. Therefore, in fitting this function to the data for the shear modulus from the three experiments, we further constrained the shift factors to have a similar temperature dependence, with $\log[b(T)] = C \log[a(T)]$, where C is a constant.

We now assume a functional representation for $\lambda(t, T)$ based on $\mu(t, T)$ and data from the literature, and then examine the resulting behavior calculated for $m(t, T)$. First, we assume that $\lambda(t, T)$ follows a stretched exponential behavior that has the same time dependence as $\mu(t, T)$; in effect, we choose $\lambda(t, T) = k_1 \mu(t, T) + k_2 b(T)$, where k_1 and k_2 are constants to be determined and $b(T)$ is the vertical shift factor used in the model for $\mu(t, T)$ in Eq. (19). The functional form for $\lambda(t, T)$ is therefore given by:

$$\lambda(t, T) = b(T) \left(k_1 [\mu_0 - \mu_\infty] \exp \left\{ - \left[\frac{t}{a(T)\tau} \right]^\beta \right\} + k_1 \mu_\infty + k_2 \right), \quad (20)$$

where μ_0 , μ_∞ , β , and τ are the same parameters in Eq. (19). The constants k_1 and k_2 are determined by matching the behavior of $\lambda(t, T)$ and $\mu(t, T)$ to data for the bulk modulus and Poisson's ratio found in the literature. In the linearized theory of elasticity, the Lamé constants λ and μ are combined to calculate the bulk modulus $K = (3\lambda + 2\mu)/3$ and Poisson's ratio $\nu = \lambda/[2(\lambda + \mu)]$. For time-dependent and temperature-dependent viscoelastic behavior, the bulk modulus relation is only altered to include the dependence on time and temperature, with $K(t, T) = [3\lambda(t, T) + 2\mu(t, T)]/3$, but Poisson's ratio $\nu(t, T)$ is not simply equal to $\lambda(t, T)/\{2[\lambda(t, T) + \mu(t, T)]\}$, as shown by Tschoegl (1989). Using the viscoelastic correspondence principle (under isothermal conditions), Tschoegl demonstrates that $\nu(t, T)$ is the inverse Laplace transform of a ratio of functions involving the Laplace transforms of $\lambda(t, T)$ and $\mu(t, T)$, so that it is not a function that can be calculated in closed form, in general. However, Tschoegl also shows that the simple algebraic relation holds in the limit of very short times, with $\nu(0, T) = \lambda(0, T)/\{2[\lambda(0, T) + \mu(0, T)]\}$, and also holds in the limit of very long times, with $\nu(\infty, T) = \lambda(\infty, T)/\{2[\lambda(\infty, T) + \mu(\infty, T)]\}$. We choose a value for $\nu(0, T)$ to relate

$\lambda(0,T)$ to $\mu(0,T)$. We also choose a value for the ratio of the bulk modulus at infinite times to the bulk modulus at zero time, $K(\infty,T)/K(0,T)$, to determine $\lambda(\infty,T)$. Data from the literature indicate that $\nu(t,T)$ remains nearly constant with a value of 0.30 [Ferry (1961)], so we first assume that $\nu(0,T) = 0.30$. The literature also indicates that the relative decrease in the bulk modulus $K(t,T)$ is much less than the relative decrease in the shear modulus $\mu(t,T)$ [Ferry (1961,1980); McKinney and Belcher (1963)]. We assume that the relative change in the magnitude of the bulk modulus is the same as that reported by McKinney and Belcher (1963) for dynamic measurements on poly(vinyl acetate) at the midpoint of the temperature range they investigated (50 °C) and at atmospheric pressure; the relevant data are shown in a figure that is also reproduced in the later edition of the book by Ferry (1980). For those data, $K(\infty,50^\circ\text{C})/K(0,50^\circ\text{C}) = 0.59$; McKinney and Belcher (1963) suggest a linear dependence on temperature for both $K(\infty,T)$ and $K(0,T)$, so that $K(\infty,T)/K(0,T)$ at atmospheric pressure varies from 0.64 to 0.56 as the temperature changes from 0 to 100 °C. With the choices of $\nu(0,T) = 0.30$ and $K(\infty,T)/K(0,T) = 0.59$, the constants k_1 and k_2 are calculated as

$$k_1 = \frac{0.665\mu_0 + 2\mu_\infty}{3(\mu_0 - \mu_\infty)}, \quad (21)$$

$$k_2 = \left(\frac{3}{2} - k_1\right)\mu_0,$$

where μ_0 and μ_∞ are the parameters fit to the shear modulus data in Eq. (19). Note that by choosing $\lambda(t,T) = k_1\mu(t,T) + k_2b(T)$, both $\nu(0,T)$ and $K(\infty,T)/K(0,T)$ are actually independent of temperature.

The calculated modulus functions $m(t,T)$ and $n(t,T)$ are also fit to equations of the same form as Eq. (19), using the same $a(T)$ determined from the shear modulus data. The higher-order modulus functions $m(t,T)$ and $n(t,T)$ are given by

$$m(t,T) = b_m(T) \left([m_0 - m_\infty] \exp \left\{ - \left[\frac{t}{a(T)\tau_m} \right]^{\beta_m} \right\} + m_\infty \right), \quad (22)$$

$$n(t,T) = b_n(T) \left([n_0 - n_\infty] \exp \left\{ - \left[\frac{t}{a(T)\tau_n} \right]^{\beta_n} \right\} + n_\infty \right). \quad (23)$$

The exponents β_m and β_n and the characteristic relaxation times τ_m and τ_n are parameters fit to the data for each higher-order modulus function, as are the parameters governing the initial values (m_0 and n_0) and terminal values (m_∞ and n_∞) for each function. Each modulus function is also allowed a different vertical shift factor [$b_m(T)$ and $b_n(T)$], which are again constrained to have temperature dependence similar to that of $a(T)$, so that $\log[b_m(T)] = C_m \log[a(T)]$ and $\log[b_n(T)] = C_n \log[a(T)]$. The constants C , C_m , and C_n were all allowed to differ in the current work.

The convolution integrals in Eqs. (17) and (18) are approximated as summations over step changes in $D(t,T)$ [calculated from the measured volumetric strain $\delta(t,T)$], with the time-shifted moduli evaluated using the functions given in Eqs. (19) and (20). We assume that the step from D_i to D_{i+1} takes place at the midpoint of the interval between t_i and t_{i+1} . The first step from $D_0 = 0$ to D_1 is applied at $t = 0$, since the time origin has been specified to lie at the midpoint of the step during which the twist is applied, as noted earlier. The convolution integral in Eq. (17) up to a time t_k therefore takes the form

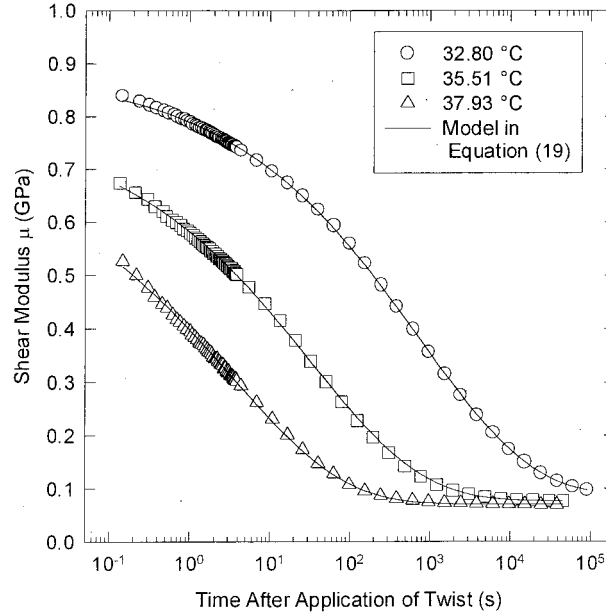


FIG. 4. Symbols are the shear modulus $\mu(t, T)$ for experiments at 32.80, 35.51, and 37.93 °C, calculated using Eq. (16). Solid lines indicate the model in Eq. (19), with the calculated model parameters listed in Table I.

$$\int_0^{t_k} \mu(t-\xi, T) \frac{\partial D(\xi, T)}{\partial \xi} d\xi \approx \mu(t_k, T) D_1(T) + \sum_{i=2}^k \mu \left[t_k - \left(\frac{t_i + t_{i+1}}{2} \right), T \right] [D_i(T) - D_{i+1}(T)] \quad (24)$$

with the convolution integral in Eq. (18) evaluated similarly. This process can be inverted to calculate $D(t, T)$ if the value of the convolution integral is known at each time t_i along with the functional representation of $\mu(t, T)$. Thus, if $\lambda(t, T)$, $\mu(t, T)$, $m(t, T)$, and $n(t, T)$ are known, $D(t, T)$ can be calculated using Eq. (14), and then $N(t, T)$ calculated using Eq. (15).

IV. RESULTS AND DISCUSSION

Data for the shear modulus $\mu(t, T)$ are plotted in Fig. 4, as calculated from the measured moment $M(t, T)$ using Eq. (16) with $\psi = 3.94 \text{ rad/m}$ and $R_0 = 15.22 \text{ mm}$. The data come from experiments at 37.93, 35.51, and 32.80 °C. The standard uncertainty in $\mu(t, T)$ is calculated using the propagation of uncertainties to be $0.002 \text{ GPa} + 0(0.03)\mu(t, T)$. The model from Eq. (19) is also shown in the figure as the solid lines, and it can be seen that the agreement with the data is very good. The calculated model parameters are listed in Table I. DiMarzio and Yang (1997) have recently presented a theory suggesting that the time-temperature shift factor at equilibrium below the glass transition should follow an Arrhenius relation. The shift factor $a(T)$ can be fit very well with an Arrhenius equation, giving an activation energy for $a(T)$ of 836 kJ/mol (standard uncertainty 46 kJ/mol). O'Connell and McKenna (1999) investigated the theory of DiMarzio and Yang (1997) using a polycarbonate aged into equilibrium below the glass transition temperature and found the activation energy for $a(T)$ of the polycarbonate to be 958 kJ/mol. Over this small temperature range, the log of the shift factors are equally

TABLE I. Parameters for $\mu(t, T)$ in Eq. (19).

Parameter	Value	Standard uncertainty
μ_0	0.7888 GPa	0.0022 GPa
μ_∞	0.0768 GPa	0.0005 GPa
β	0.3067	0.0013
τ	32.39 s	0.36 s
$a(32.80^\circ\text{C})$	23.00	0.28
$a(35.51^\circ\text{C})$	1	...
$a(37.93^\circ\text{C})$	0.1030	0.0006
$b(32.80^\circ\text{C})$	1.125	0.002
$b(35.51^\circ\text{C})$	1	...
$b(37.93^\circ\text{C})$	0.918	0.001
Root-mean-square difference between data and model (GPa)	0.002 56 GPa	...

well represented as linear functions of T , with $\log[a(T)] = (-0.459 \text{ K}^{-1})(T - T_R)$ with standard uncertainty in the slope of 0.027 K^{-1} , and $\log[b(T)] = (-0.0173 \text{ K}^{-1})(T - T_R)$ with standard uncertainty in the slope of 0.0010 K^{-1} . T_R is the reference temperature of 35.51°C .

The function $\lambda(t, T)$ is specified by Eqs. (20) and (21), along with the parameters for $\mu(t, T)$ given in Table I. The constants k_1 and k_2 are calculated to be $k_1 = 0.318$ and $k_2 = 0.933$ GPa. The standard uncertainty in $\lambda(t, T)$ is assumed to be k_1 times the standard uncertainty in $\mu(t, T)$.

The choices made for the description of $\lambda(t, T)$ result in a Poisson's ratio that increases steadily with time from $\nu(0, T) = 0.30$ to $\nu(\infty, T) = 0.46$, independent of the temperature. This behavior is consistent with experimental results in the literature [Wine-man and Rajagopal (2000)].

The negative of the higher-order modulus function $n(t, T)$ calculated using Eq. (17) is plotted as symbols in Fig. 5, along with solid lines that are fit to the model in Eq. (23). The parameters fit to the data for $n(t, T)$ are listed in Table II. It can be seen that $n(t, T)$ is a monotonic, negative function that is about one order of magnitude larger than $\mu(t, T)$. Both terms in Eq. (17) are important, especially at short times, where they are of similar magnitude. The standard uncertainty in $n(t, T)$ is calculated to be $0.1 \text{ GPa} - (0.04)n(t, T)$.

The function chosen for $\lambda(t, T)$ was input to Eq. (18) along with the experimental data to calculate the other higher-order modulus function $m(t, T)$. The negative of that function is plotted in Fig. 6, and it can be seen that $m(t, T)$ is also a monotonic, negative function that is about one order of magnitude larger than $\mu(t, T)$, similar to $n(t, T)$. As with $n(t, T)$, all of the terms in Eq. (19) make contributions of similar magnitude, especially at shorter times. The standard uncertainty in $m(t, T)$ is calculated to be $0.1 \text{ GPa} - (0.02)m(t, T)$. These data for $m(t, T)$ were fit twice, first fitting all the data without weighting, and then weighting the data at 32.80°C between 10 and 10^4 s to have one tenth the influence of the other data, so as to lessen the influence of the hump in that curve. The parameters for the unweighted fit are listed in Table III, and the parameters for the weighted fit are listed in Table IV. The difference between the two curves is not very great in this plot of $m(t, T)$, but the difference is greatly magnified in the subsequent calculation of the volumetric strain, as shown later. The weighted fit captures all of the

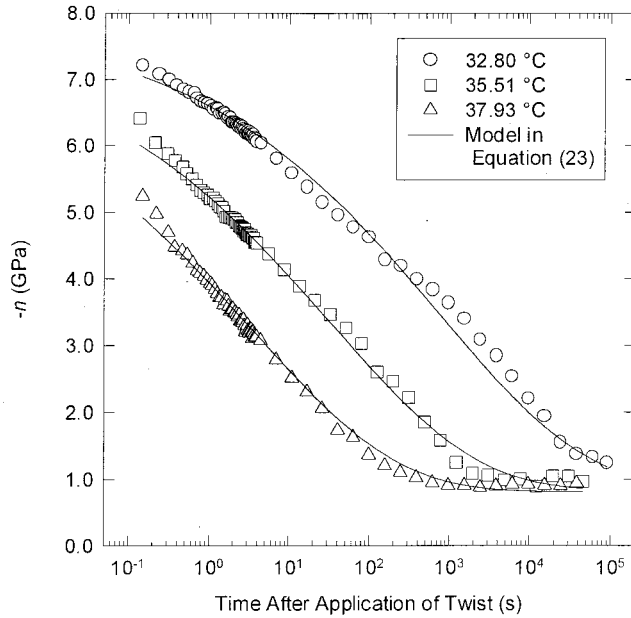


FIG. 5. Symbols are the negative of the higher-order modulus function $n(t, T)$ calculated using Eq. (17) for the experiments at 32.80, 35.51, and 37.93 °C. Solid lines indicate the model in Eq. (23), with the calculated model parameters listed in Table II.

behavior at the two higher temperatures better, and also captures the initial part of the relaxation at all three temperatures better. The unweighted fit is strongly influenced by the nonmonotonic volume relaxation behavior at 32.80 °C, which is not apparent at the higher temperatures. The relaxation behavior at 32.80 °C might be evidence of an additional relaxation mechanism [Read (1992); Perez *et al.* (1999)], but this calculation for $m(t, T)$ is somewhat exploratory without a direct measurement of $\lambda(t, T)$. The effects of some different choices for $\lambda(t, T)$ on $m(t, T)$ were not very great, as discussed later. Also, note that the evidence for an additional relaxation mechanism appears only in the normal force and volume change, which are nonlinear responses to the torsion. The shear modulus can be superposed quite well at all temperatures. No evidence of a β mechanism [Read (1992); Perez *et al.* (1999)] was reported in earlier investigations with this material

TABLE II. Parameters for $n(t, T)$ in Eq. (23).

Parameter	Value	Standard uncertainty
n_0 (GPa)	-7.620 GPa	0.096 GPa
n_∞ (GPa)	-0.834 GPa	0.023 GPa
β_n	0.2368	0.0046
τ_n	33.1 s	1.8 s
$b_n(32.80 \text{ }^\circ\text{C})$	1.038	0.003
$b_n(35.51 \text{ }^\circ\text{C})$	1	...
$b_n(37.93 \text{ }^\circ\text{C})$	0.973	0.002
rms difference between data and model	0.104 GPa	...

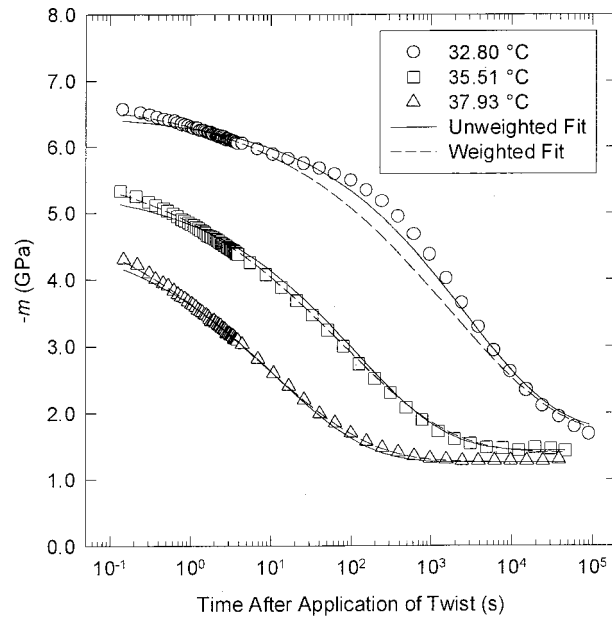


FIG. 6. Symbols are the negative of the higher-order modulus function $m(t, T)$ calculated using Eq. (18) for the experiments at 32.80, 35.51, and 37.93 °C. Solid lines are fit to the model in Eq. (22) with all data having the same weight; the calculated model parameters for this case are listed in Table III. Dashed lines are fit to the model in Eq. (22) with the data at 32.80 °C between 10 and 10^4 s weighted to have one tenth the influence of the other data; the calculated model parameters for this case are listed in Table IV.

[Duran and McKenna (1990); Santore *et al.* (1991); McKenna *et al.* (1994, 1995); Schultheisz *et al.* (1995), Lee and McKenna (1988)] using the torsional dilatometer or other types of experiments. This is consistent with the superposability of the shear modulus measured in the present series of experiments. Lee and McKenna (1988) performed stress relaxation experiments with this epoxy in uniaxial tension at a strain of 0.0025 and found no evidence of a β mechanism. However, the relaxation behavior of the uniaxial Young's modulus should be governed largely by the relaxation behavior of the shear modulus component, which shows no evidence of a second relaxation mechanism in this investigation. In addition, nonlinear material behavior such as the normal force and volume change in the torsion experiments could be imperceptible at a strain level of

TABLE III. Parameters for unweighted fit of $m(t, T)$ in Eq. (22).

Parameter	Value	Standard uncertainty
m_0	-6.382 GPa	0.037 GPa
m_∞	-1.864 GPa	0.017 GPa
β_m	0.4106	0.0066
τ_m	132.6 s	3.6 s
$b_m(32.80 \text{ }^\circ\text{C})$	1.217	0.003
$b_m(35.51 \text{ }^\circ\text{C})$	1	...
$b_m(37.93 \text{ }^\circ\text{C})$	0.868	0.001
rms difference between data and model	0.0939 GPa	...

TABLE IV. Parameters for weighted fit of $m(t, T)$ in Eq. (22).

Parameter	Value	Standard uncertainty
m_0	-6.876 GPa	0.035 GPa
m_∞	-1.814 GPa	0.011 GPa
β_m	0.3308	0.0039
τ_m	89.6 s	2.2 s
$b_m(32.80\text{ }^\circ\text{C})$	1.170	0.002
$b_m(35.51\text{ }^\circ\text{C})$	1	...
$b_m(37.93\text{ }^\circ\text{C})$	0.893	0.001
Weighted rms difference between data and model	0.0544 GPa	...
Unweighted rms difference between data and model	0.139 GPa	...

0.0025. The previous work with the torsional dilatometer did not extend to modeling the normal force and volume change associated with the torsion [Duran and McKenna (1990); Santore *et al.* (1991); McKenna *et al.* (1994, 1995); Schultheisz *et al.* (1995)]. Using the functional representations for $\lambda(t, T)$, $\mu(t, T)$, $m(t, T)$, and $n(t, T)$ given in Eqs. (19), (20), (22), and (23), along with the parameters in Tables I–IV, predictions of the moment, the normal force and the volumetric strain can be calculated through Eqs. (11), (14), and (15). Figure 4 represents the comparison between the experimental data and the model for the moment (or torque), and the agreement between experiment and model is very good. The experimental data for the normal force and the volumetric strain along with the corresponding model predictions are compared in Figs. 7 and 8. Both the weighted and unweighted fits for $m(t, T)$ have been used to calculate model predictions. The normal force is governed primarily by $n(t, T)$, and so the difference between the weighted and unweighted model predictions is small. Most of the differences between the model and the experimental data for the normal force mirrors the differences between the calculated $n(t, T)$ and the fit to $n(t, T)$, which might be reduced by adding more terms to improve the fit. Using a sum of exponentials instead of a single stretched exponential would allow for more complexity in the function, but would require a much larger number of parameters. The normalized volume change $\delta(t, T) = [V(t, T) - V_{\text{ref}}(T)]/V_{\text{ref}}(T)$ is governed primarily by the function $m(t, T)$, as can be seen by the differences between the weighted and unweighted models in Fig. 8. The weighted model matches the experiments well at 35.51 and 37.93 °C, but cannot fit the peak at 32.80 °C. The unweighted model captures some aspect of the peak in the volume response at 32.80 °C, but reduces the agreement with the experiment in other areas. Again, the single stretched exponential function is fairly restrictive, and a function with more parameters might be more successful in modeling the data. However, the good agreement at the higher temperatures for the weighted model again suggests that a separate mechanism could be acting at 32.80 °C.

An alternative method for looking at the time-temperature behavior of the nonlinear response is through direct superposition of the normal force measurements in Fig. 7 (clearly the volume responses in Fig. 8 cannot be superposed). Superposing the normal force allows for calculation of a temperature shift factor $a_{\text{NF}}(T)$ and a vertical shift factor $b_{\text{NF}}(T)$. Fitting $a_{\text{NF}}(T)$ to an Arrhenius equation gives an activation energy of 934 kJ/mol (standard uncertainty 90 kJ/mol), or as a linear function of T , $\log[a_{\text{NF}}(T)] = (-0.512\text{K}^{-1})(T - T_R)$ with standard uncertainty in the slope of 0.052K^{-1} . T_R is the reference temperature of 35.51 °C. The multiplicative vertical shift factor $b_{\text{NF}}(T)$ was

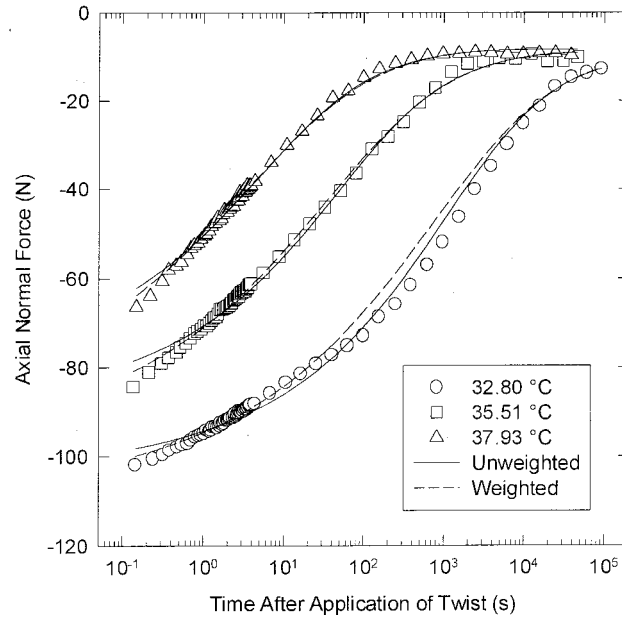


FIG. 7. Symbols are the measured data for the axial normal force for the experiments at 32.80, 35.51, and 37.93 °C. The lines are the corresponding model predictions calculated from Eqs. (14) and (15) using the functions for $\lambda(t, T)$, $\mu(t, T)$, $m(t, T)$, and $n(t, T)$ given in Eqs. (19), (20), (22), and (23). Solid lines use the unweighted fit for $m(t, T)$ (parameters in Table III); dashed lines use the weighted fit for $m(t, T)$ (parameters in Table IV).

found to be $\log[b_{\text{NF}}(T)] = (-0.0112 \text{ K}^{-1})(T - T_R)$ with standard uncertainty in the slope of 0.0011 K^{-1} . The time-temperature shift factor for the normal force has a somewhat greater dependence on the temperature than that for the shear modulus $\mu(t, T)$. This result is consistent with the shift of the normal force relaxation to later times (as compared to the torque) with decreasing temperature, as seen in Figs. 1–3.

The key to the extended relaxation and nonmonotonic behavior for volumetric strain $\delta(t, T)$ within the context of this model is the longer time scale and broader spectrum of $m(t, T)$ as compared to $\lambda(t, T)$ and $\mu(t, T)$. In order to match the relaxation of the higher-order modulus functions $[-4m(t, T) + n(t, T)]$ that appear on the right-hand side of Eq. (14), the relaxation of $\delta(t, T)$ [$\approx D(t, T)$ in the equation] must be slowed or reversed to affect the convolution with $[\lambda(t, T) + \mu(t, T)]$ on the left-hand side in the appropriate way. Results from an experiment using only a single twist step suggest that the volume change caused by the torsion dissipates entirely at long times, meaning that $\delta(t, T)$ will eventually approach zero. This behavior might be expected, since the shear modulus decreases much more than the bulk modulus, so that at long times the polymer responds more like an incompressible material. For the parameters used to model $\lambda(t, T)$ and $\mu(t, T)$, Poisson's ratio at long times approaches $\nu(\infty, T) = 0.46$, independent of temperature. Within the context of Murnaghan's analysis, however, this result implies that the terminal values of the modulus functions are related, so that the quantity $\{-4[\lambda(\infty, T) + 2\mu(\infty, T) + m(\infty, T)] + n(\infty, T)\}$ should also approach zero. This condition was not enforced here. The choice we have made for $\lambda(t, T)$ is representative of the general behavior of polymers, but we also briefly examined the influence of different choices for $\lambda(t, T)$ on the resulting calculation for $m(t, T)$ [Schultheisz and McKenna (1999)]. We

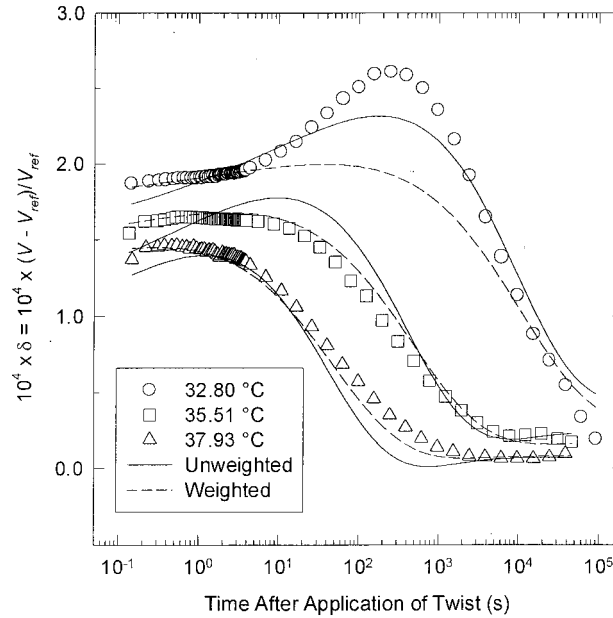


FIG. 8. Symbols are the measured data for $\delta(t, T) = [V(t, T) - V_{\text{ref}}(T)]/V_{\text{ref}}(T)$ for the experiments at 32.80, 35.51, and 37.93 °C. The lines are the corresponding model predictions calculated from Eq. (14) using the functions for $\lambda(t, T)$, $\mu(t, T)$, $m(t, T)$, and $n(t, T)$ given in Eqs. (19), (20), (22), and (23). Solid lines use the unweighted fit for $m(t, T)$ (parameters in Table III); dashed lines use the weighted fit for $m(t, T)$ (parameters in Table IV).

investigated two forms for $\lambda(t, T)$: first, $\lambda = \text{constant}$, and second, $\lambda(t, T) = C\mu(t, T)$, with C a constant. The constant in either case was determined by specifying Poisson's ratio at time $t = 0$, which was also used in defining $\lambda(t, T)$ in Eqs. (20) and (21). These two choices represent rough limits on the expected behavior of $\lambda(t, T)$. In the first case, with $\lambda = \text{constant}$, Poisson's ratio is a slightly increasing function of time and the relative decrease in the bulk modulus is minimized; this case is equivalent to assuming that the relaxation behavior of λ lies outside the time of the measurements. In the second case, with $\lambda(t, T) = C\mu(t, T)$, Poisson's ratio is nearly constant, and the relative change in the bulk modulus is equal to the relative change in the shear modulus $\mu(t, T)$, since the bulk modulus is then also a multiple of $\mu(t, T)$. For either of these limit cases, $m(t, T)$ is still found to be a monotonic function of time, which is negative and about an order of magnitude larger than $\mu(t, T)$, similar to the result in Fig. 6. The most significant difference between these limit cases is that the magnitude of the relaxation of $\lambda(t, T)$ during the time of the experiments changes by approximately one decade, which leads to a change of similar magnitude in the terminal behavior of $m(t, T)$. The choice for $\lambda(t, T)$ in the present paper lies between the two limit cases. Changing the magnitude of $\lambda(t, T)$ (by choosing a different value of Poisson's ratio at $t = 0$) would lead to a corresponding shift in the magnitude of $m(t, T)$. Shifting the characteristic relaxation time of $\lambda(t, T)$ by one or two decades either way also does not have a significant impact on $m(t, T)$. Conversely, assuming a behavior for $m(t, T)$ to calculate $\lambda(t, T)$ appears to be an unstable process in that small changes in $m(t, T)$ can cause large, physically unreasonable results for $\lambda(t, T)$.

It does not appear to be possible to determine $\lambda(t, T)$ and $m(t, T)$ unambiguously from the torsional deformation alone, such as by mapping out the variations in the measurements as functions of strain level and/or cylinder radius. A separate test in a different geometry could be used to evaluate the different modulus functions and validate the model. A simple shear test would lead to equations that involve the same four modulus functions $\lambda(t, T)$, $\mu(t, T)$, $m(t, T)$, and $n(t, T)$, but in different combinations. A uniaxial stress relaxation test of the cylinder in which the axial strain was imposed and the axial stress and the transverse strains were measured (in conjunction with the torsion test) would provide two equations in addition to Eqs. (16), (17), and (18), giving five equations involving the five modulus functions that arise from Murnaghan's analysis: $\lambda(t, T)$, $\mu(t, T)$, $l(t, T)$, $m(t, T)$, and $n(t, T)$. It is not possible to perform such a test in the torsional dilatometer, so it would be important to ensure that the materials and thermal histories for the different tests matched closely.

For simple shear of a sample where the lateral faces are free to expand or contract, the model predicts behavior similar to that found in the torsional deformation. The shear stress would be the same as in the linearized theory, the normal stress would relax on a time scale similar to the shear stress, and the volume change would demonstrate extended, nonmonotonic relaxation. Similarly, for torsion of a cylinder in which the ends are free to move, the net volumetric strain is predicted to be nearly the same as for the case where the ends are fixed. In this situation, the axial strain is predicted to be positive and nearly constant with time, while the radial strain would be initially close to zero but increasingly negative with time until it offsets the axial strain.

Our findings that both $m(t, T)$ and $n(t, T)$ are negative and about an order of magnitude larger than $\mu(t, T)$ are consistent with experimental results of Bridgman (1948) as examined by Murnaghan (1951) within the context of his theory. Bridgman (1948) investigated the hydrostatic compression of the metal sodium. For those data, Murnaghan calculated that the parameter $(9l + n)$ was negative and approximately 190 times larger in magnitude than $(3\lambda + 2\mu)$, where l is the third of the higher-order elastic constants in the theory, which does not play a role in the case of torsional deformation. One might expect that these higher-order parameters must be larger than the Lamé constants because they multiply the strains raised to the second power to give stresses, with the strains being small quantities within the range of applicability of Murnaghan's formulation.

In the torsion problem, the magnitude of the strain is governed by ψ , the angle of twist per unit length of the cylinder, and from Eqs. (11), (14), and (15), it can be seen that the moment only includes a term linear in ψ and the normal force and radial expansion include only terms in ψ^2 . The behavior that can be described by the theory is thus limited by truncating the series solutions to terms of order lower than ψ^3 . The series could be extended to include additional terms to capture nonlinearity in the moment with increasing ψ . Earlier work by Duran and McKenna (1990) suggests that the strain level used for the testing in this report is still in the regime where the torque is a nearly linear function of the strain, so the single term in the shear modulus is sufficient to describe the torque response. The moment M is an odd function of ψ , so M would include only odd powers of ψ , while the normal force and radial expansion are even functions of ψ , and so would include only even powers of ψ . Extending the series to terms of order ψ^3 would allow for nonlinearity in the moment, but would introduce four additional parameters in Murnaghan's solution. Similarly, extending the series to terms of order ψ^4 would allow for more flexibility in describing the normal force and radial expansion, but would introduce another five parameters. This procedure might be feasible, given sufficient data on the

torque, normal force and volume change as a function ψ , but evaluating all the new parameters separately would be impossible without other experiments in addition to the torsion tests.

For the experiments reported in the present paper, the analysis of the nonlinear response to the torsional deformation may be complicated by the effects of the temperature jumps, which were used to investigate the relation between volume recovery and physical aging. More accurate measurements of the material response to the torsion could be made by first allowing the sample to reach thermal equilibrium (and possibly thermodynamic equilibrium) before making the connection between the sample grip and the motor, as was done in an earlier investigation with the torsional dilatometer [Duran and McKenna (1990)]. The scaling of the calculated material properties for the present model could also be more thoroughly investigated by varying the angle of twist per unit length ψ , which has also been done in previous experiments [Duran and McKenna (1990); Santore *et al.* (1991)]. The previous studies used different methods of analyzing the data [Duran and McKenna (1990); Santore *et al.* (1991); Waldron *et al.* (1995)].

V. CONCLUSIONS

The NIST torsional dilatometer has been used to make simultaneous measurements of the torque, axial normal force, and volume change in response to a torsional deformation of an epoxy cylinder that was aged into equilibrium at temperatures approximately 5–10 °C below the nominal glass transition temperature. The range of observed relaxation behaviors is quite rich. In response to the torsional deformation, the torque and axial normal force behaved as expected, decaying monotonically over time, but the volume change displayed an extended relaxation that varies with temperature and shows a significant nonmonotonic decay at the lowest temperature investigated. This nonmonotonic volume change has not been reported previously.

We modified Murnaghan's (1951) series expansion solution for torsion of compressible materials in two ways. First, we extended the solution to torsion of a cylinder with fixed ends. More importantly, we followed the suggestion of Rivlin (1956) that isochronal data from stress relaxation experiments can be treated as elastic data. We constructed viscoelastic forms for the Murnaghan nonlinear modulus terms.

Our results demonstrate that, upon using classical concepts such as time-temperature superposition, and assuming that the modulus functions in the Murnaghan model are monotonic functions in time, we can reproduce qualitatively the nonmonotonic nature of the volume response in torsion observed in the epoxy at the lowest measurement temperature. While this result does not "explain" the mechanism of the nonmonotonic volume relaxation, it moves the observation to a level of the nature of the continuum relaxation functions.

Finally, we suggest that further investigation is required to provide a quantitative description of the observed results. This implies the need for more complete models for compressible material viscoelasticity than are currently available as well as more experimentation in the NIST torsional dilatometer that is combined with experiments in other geometries of deformation such as uniaxial extension with direct measurement of the lateral strains.

References

- Baker, M and J. L. Ericksen, "Inequalities restricting the form of the stress-deformation relations for isotropic elastic solids and Reiner–Rivlin fluids," *J. Wash. Acad. Sci.* **44**, 33–35 (1954).
- Bridgman, P. W., "The compression of 39 substances to 100,000 KG/CM²," *Proc. Am. Acad. Arts Sci.* **76**, 55–70 (1948).
- Colucci, D. M., P. A. O'Connell, and G. B. McKenna, "Stress relaxation experiments in polycarbonate: a comparison of volume changes for two commercial grades," *Polym. Eng. Sci.* **37**, 1469–1474 (1997).
- CRC Handbook of Chemistry and Physics*, 78th ed., edited by D. R. Lide (CRC Press, Boca Raton, FL, 1997), pp. 6–133.
- DiMarzio, E. A. and A. J. M. Yang, "Configurational entropy approach to the kinetics of glasses," *J. Res. Natl. Inst. Stand. Technol.* **102**, 135–157 (1997).
- Duran, R. S. and G. B. McKenna, "A torsional dilatometer for volume change measurements on deformed glasses: Instrument description and measurements on equilibrated glasses," *J. Rheol.* **34**, 813–839 (1990).
- Ferry, J. D., *Viscoelastic Properties of Polymers* (Wiley, New York, 1961).
- Ferry, J. D., *Viscoelastic Properties of Polymers*, 3rd ed. (Wiley, New York, 1980).
- Green, A. E., "Finite elastic deformation of compressible isotropic bodies," *Proc. R. Soc. London, Ser. A* **227**, 271–278 (1955).
- Hodge, I. M., "Enthalpy relaxation and recovery in amorphous materials," *J. Non-Cryst. Solids* **169**, 211–266 (1994).
- Hoger, A., "A second order constitutive theory for hyperelastic materials," *Int. J. Solids Struct.* **36**, 847–868 (1999).
- Kovacs, A. J., "Transition vitreuse dans les polymeres amorphes. Etude Phenomenologique," *Fortschr. Hochpolym.-Forsch.* **3**, 394–507 (1963).
- Kovacs, A. J., J. J. Aklonis, J. M. Hutchinson, and A. R. Ramos, "Isobaric volume and enthalpy recovery of glasses. II. A transparent multiparameter theory," *J. Polym. Sci., Polym. Phys. Ed.* **17**, 1097–1162 (1979).
- Lee, A. and G. B. McKenna, "Effect of crosslink density on physical ageing of epoxy networks," *Polymer* **29**, 1812–1817 (1988).
- Levinson, M., "Finite torsion of slightly compressible rubberlike circular cylinders," *Int. J. Non-Linear Mech.* **7**, 445–463 (1972).
- McKenna, G. B. and L. J. Zapas, "The time dependent strain potential function for a polymeric glass," *Polymer* **26**, 543–550 (1985).
- McKenna, G. B., "Glass formation and glassy behavior," in *Comprehensive Polymer Science*, 2, *Polymer Properties*, edited by C. Booth and C. Price (Pergamon, Oxford, 1989), Chap. 10, pp. 311–362.
- McKenna, G. B., C. R. Schultheisz, and Y. Leterrier, "Volume recovery and physical aging: dilatometric evidence for different kinetics," *Deformation, Yield and Fracture of Polymers*, Proceedings of the 9th International Conference, Cambridge, UK, 1994, paper 31/1.
- McKenna, G. B., Y. Leterrier, and C. R. Schultheisz, "The evolution of material properties during physical aging," *Polym. Eng. Sci.* **35**, 403–410 (1995).
- McKenna, G. B., M. G. Vangel, A. L. Rukhin, S. D. Leigh, B. Lotz, and C. Straupe, "The τ_{eff} paradox revisited: an extended analysis of Kovacs' volume recovery data on poly(vinyl acetate)," *Polymer* **40**, 5183–5205 (1999).
- McKinney, J. E. and H. V. Belcher, "Dynamic compressibility of poly(vinyl acetate) and its relation to free volume," *J. Res. Natl. Bur. Stand., Sect. A* **67A**, 43–53 (1963).
- Mijovic, J., L. Nicolais, A. D'Amore, and J. M. Kenny, "Principal features in glassy polymers. A review," *Polym. Eng. Sci.* **34**, 381–389 (1994).
- Murnaghan, F. D., *Finite Deformation of an Elastic Solid* (Wiley, London, 1951).
- O'Connell, P. A. and G. B. McKenna, "Arrhenius-type temperature dependence of the segmental relaxation below T_g ," *J. Chem. Phys.* **110**, 11054–11060 (1999).
- Penn, R. W. and E. A. Kearsley, "The scaling law for finite torsion of elastic cylinders," *Trans. Soc. Rheol.* **20**, 227–238 (1976).
- Perez, J., J. Y. Cavaille, and L. David, "New experimental features and revisiting the α and β mechanical relaxation in glasses and glass-forming liquids," *J. Mol. Struct.* **479**, 183–194 (1999).
- Pesce, J.-J. and G. B. McKenna, "Prediction of the sub-yield extension and compression responses of glassy polycarbonate from torsional measurements," *J. Rheol.* **41**, 929–942 (1997).
- Pixa, R., V. Le Dû, and C. Wippler, "Dilatometric study of deformation induced volume increase and recovery in rigid PVC," *Colloid Polym. Sci.* **266**, 913–920 (1988).
- Read, B. E., "Creep of glassy polymers in the α - and β -retardation regions. Physical aging and nonlinear behavior," *J. Rheol.* **36**, 1719–1736 (1992).
- Rivlin, R. S., "Large elastic deformation of isotropic materials IV. Further developments of the general theory," *Philos. Trans. R. Soc. London, Ser. A* **A241**, 379–397 (1948).
- Rivlin, R. S., "The solution of problems in second order elasticity theory," *J. Rational Mechanics and Analysis* **2**, 53–81 (1953).

- Rivlin, R. S., "Stress-relaxation in incompressible elastic materials at constant deformation," *Q. Appl. Math.* **14**, 83–89 (1956).
- Santore, M. M., R. S. Duran, and G. B. McKenna, "Volume recovery in epoxy glasses subjected to torsional deformations: the question of rejuvenation," *Polymer* **32**, 2377–2381 (1991).
- Scherer, G. W., *Relaxation in Glass and Composites* (Wiley, New York, 1986).
- Schultheisz, C. R., D. M. Colucci, G. B. McKenna, and J. M. Caruthers, "Modeling the differing time scales of structural recovery and mechanical relaxation observed in aging experiments," in *Mechanics of Plastics and Plastic Composites MD-68/AMD-215*, edited by M. C. Boyce (American Society of Mechanical Engineers, New York, 1995), pp. 251–282.
- Schultheisz, C. R. and G. B. McKenna, "Simultaneous measurement of torque, axial force and volume change in the torsional dilatometer and the implications for constitutive modeling," in Proceedings of the Fourth International Conference on Constitutive Laws for Engineering Materials: Experiment, Theory, Computation and Applications, Rensselaer Polytechnic Institute, Troy, NY, July 1999.
- Smith, T. L., G. Levita, and W. K. Moonan, "Reversal and activation of physical aging by applied deformations in simple compression and extension," *J. Polym. Sci., Part B: Polym. Phys.* **26**, 875–881 (1988).
- Spencer, A. J. M., *Continuum Mechanics* (Longman, New York, 1980).
- Struik, L. C. E., *Physical Aging in Amorphous Polymers and Other Materials* (Elsevier, Amsterdam, 1978).
- Struik, L. C. E., "On volume-recovery theory: 1. Kovacs' τ_{eff} paradox," *Polymer* **38**, 4677–4685 (1997a).
- Struik, L. C. E., "On volume-recovery theory: 2. Test on Kovacs's original δ vs t data," *Polymer* **38**, 5233–5241 (1997b).
- Tschoegl, N. W., *The Phenomenological Theory of Linear Viscoelastic Behavior* (Springer, Berlin, 1989).
- Wack, B., "Second and third-order effects in the torsion of circular tubes and rods," *J. Mécanique* **20**, 737–787 (1981).
- Wack, B., "The torsion of a tube (or a rod)—general cylindrical kinematics and some axial deformation and ratchet measurements," *Acta Mech.* **80**, 39–59 (1989).
- Waldron, W. K., Jr., G. B. McKenna, and M. M. Santore, "The nonlinear viscoelastic response and apparent rejuvenation of an epoxy glass," *J. Rheol.* **39**, 471–497 (1995).
- Wang, T. T., H. M. Zupko, L. A. Wyndon, and S. Matsuoka, "Dimensional and volumetric changes in cylindrical rods of polymers subjected to a twist moment," *Polymer* **23**, 1407–1409 (1982).
- Wineman, A. S. and G. B. McKenna, "Determination of the strain energy density function for compressible isotropic nonlinear elastic solids by torsion-normal force experiments," in *Nonlinear Effects in Fluids and Solids*, edited by M. M. Carroll and M. Hayes (Plenum, New York, 1996), pp. 339–353.
- Wineman, A. S. and K. R. Rajagopal, *Mechanical Response of Polymers* (Cambridge University Press, Cambridge).
- Wu, P. D. and E. van der Giessen, "On large-strain inelastic torsion of glassy polymers," *Int. J. Mech. Sci.* **35**, 935–951 (1993).
- Zapas, L. J. and T. Craft, "Correlation of large longitudinal deformations with different strain histories," *J. Res. Nat. Bur. Stand., Sect. A* **69A**, 541–546 (1965).